Addition of water, methanol, and ammonia to $Al_3O_3^-$ clusters: Reaction products, transition states, and electron detachment energies

Alfredo Guevara-García and Ana Martínez[a)]
Instituto de Investigaciones en Materiales, Universidad Nacional Autonoma de Mexico (UNAM), Circuito Exterior s/n, Ciudad Universitaria, P.O. Box 70-360, Coyoacán 04510, Distrito Federal Mexico

J. V. Ortiz
Department of Chemistry, Kansas State Universíty, Manhattan, Kansas 66506-3701

(Received 22 February 2005; accepted 12 April 2005; published online 6 June 2005)

Products of reactions between the book and kite isomers of $Al_3O_3^-$ and three important molecules are studied with electronic structure calculations. Dissociative adsorption of H_2O or CH_3OH is highly exothermic and proton-transfer barriers between anion-molecule complexes and the products of these reactions are low. For NH_3, the reaction energies are less exothermic and the corresponding barriers are higher. Depending on experimental conditions, $Al_3O_3^-$ (NH_3) coordination complexes or products of dissociative adsorption may be prepared. Vertical electron detachment energies of stable anions are predicted with *ab initio* electron propagator calculations and are in close agreement with experiments on $Al_3O_3^-$ and its products with H_2O and CH_3OH. Changes in the localization properties of two Al-centered Dyson orbitals account for the differences between the photoelectron spectra of $Al_3O_3^-$ and those of the product anions. © *2005 American Institute of Physics*.
[DOI: 10.1063/1.1926279]

INTRODUCTION

Reactions on metal-oxide surfaces that are exposed to aqueous solutions underline many of the bulk processes studied by earth and environmental scientists and have been exploited in a host of industrial processes.[1] Aluminum oxide minerals are ubiquitous on the earth's crust and alternative morphologies provide catalytic supports and optical waveguides in a broad range of technologies. The variety and complexity of this chemistry have stimulated efforts to understand fundamental reactions at the molecular level. With new techniques of synthesis and separation, it is possible to examine the reactivity of isolated Al_nO_m clusters. Given the pervasive presence of hydroxides on active surfaces, reactions between aluminum oxide clusters and water have been studied to identify structural and mechanistic trends.[2] Several kinds of spectrometric probes have been applied to aluminum oxide and hydroxide clusters.[3–10]

Anion photoelectron spectra[4–9] and theoretical interpretations[11–20] of them have established that more than one isomer may be generated by current techniques for the preparation of an $Al_nO_m^-$ cluster with a selected mass. Photoisomerization in $Al_3O_3^-$ was inferred by Wu *et al.* from variations in spectral peak intensities produced by changes in laser fluence and in the conditions of ion synthesis and transport.[6] Subsequent experiments demonstrated the separation of spectral components associated with two energetically close isomers.[7]

Reactions between $Al_3O_3^-$ and water molecules have been examined with mass spectrometry and the products have been characterized with anion photoelectron spectroscopy by Akin and Jarrold.[8] The presence of species with the formulas $Al_3O_3^-(H_2O)$ or $Al_3O_3^-(H_2O)_2$ (that is, $Al_3O_4H_2^-$ and $Al_3O_5H_4^-$, respectively), the relative abundance of the larger of these two clusters, and the absence of $Al_3O_3^-$ $(H_2O)_n$ species for $n \geqslant 3$ have been observed for moderate water vapor pressures. Whereas two well-separated peaks occur in the $Al_3O_3^-$ and $Al_3O_5H_4^-$ spectra, the $Al_3O_4H_2^-$ experiment yields a more subtle pair of broad, overlapping humps. These results suggest a qualitative difference in bonding between $Al_3O_4H_2^-$ and $Al_3O_3^-$.

We have previously reported[14–17] the ground-state geometries and energies of the low-lying states of neutral and anionic clusters with the formula Al_3O_n for $n=1-5$. Electron propagator calculations on vertical electron detachment energies (VEDEs) were used to assign anion photoelectron spectra. For the $Al_3O_3^-$ cluster, the existence of approximately isoenergetic book (also known as box) and kite isomers (see Fig. 1) was demonstrated by assigning calculated VEDEs of both isomers to peaks in the photoelectron spectrum.[14,16]

Computational studies[19,20] on $Al_3O_4H_2$ and $Al_3O_4H_2^-$ concluded that the book form of the anion [Fig. 2(a)] is chiefly responsible for the main features of the corresponding photoelectron spectrum and that lower symmetry in this isomer accounts for the qualitative differences between the $Al_3O_3^-$ and $Al_3O_4H_2^-$ spectra. These studies also suggested that the kite isomer [Fig. 2(b)] should not be ignored in interpreting the photoelectron spectrum, for its energy is close to that of the book isomer [Fig. 2(c)]. This result suggests that the first hump in the $Al_3O_4H_2^-$ spectrum may be shifted to slightly higher energies and broadened relative to the first book $Al_3O_3^-$ peak by the presence of a second, less stable

a)Electronic mail: martina@matilda.iimatercu.unam.mx

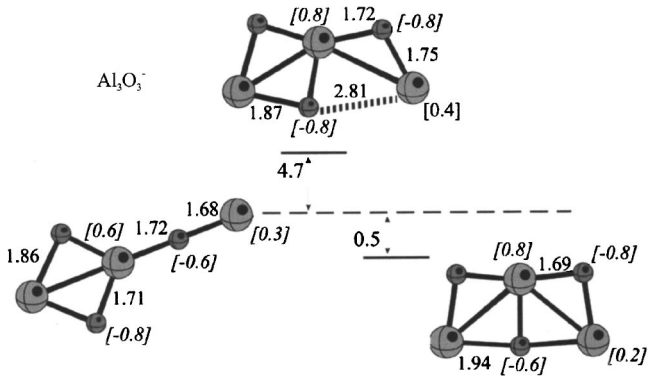

FIG. 1. B3LYP/6-311+G(2*d*,*p*) optimized structures of $Al_3O_3^-$: book and kite minima and the transition state that lies between them. Relative energies are in kcal/mol and Mulliken atomic charges are in brackets.

isomer with a somewhat larger VEDE.[19] In both structures, the two protons are bound to O atoms that are neighbors of the most centrally located Al atom.

Akin and Jarrold[8] also reported a broad and congested photoelectron spectrum for $Al_3O_3^-(CH_3OH)$ which resembled that of $Al_3O_4H_2^-$. Dissociative adsorption leading to a structure with hydroxide and methoxide ions may result.

Several unanswered questions remain for $Al_3O_3^-$ and its products with H_2O and CH_3OH. First, what is the energy barrier between the two stable isomers for $Al_3O_3^-$? Second, how does a water molecule affect the barrier for isomerization between the book and kite structures of $Al_3O_3^-$? Third, how do reactions with methanol differ from those with water? Fourth, are reactions with oxygen-free molecules such as NH_3 similar to those observed with water and methanol? To answer these questions and to gain insights into relationships between electronic structure and reactivity, we have calculated stable structures, relative energies, transition states, VEDEs, and Mulliken atomic charges.

METHODS

Geometry optimizations without symmetry constraints were performed with the GAUSSIAN03 program[21] in the B3LYP/6-311+G(2*d*,*p*) approximation.[22,23] Optimized minima and transition states were confirmed with harmonic frequency analysis. To locate transition states, the synchronous transit-guided quasi-Newton (STQN) method[24] has been used.

Previous work indicates that B3LYP/6-311+G(2*d*,*p*) optimizations are likely to provide accurate structures.[14] The most stable anionic structures from similar density-functional calculations were verified by MP2/6-311G(*d*,*p*) optimizations. No substantial structural differences between these results were found; discrepancies between bond lengths were less than 0.001 nm. Moreover, the calculations of Das *et al.*[25] on $Al_5O_4^-$ and $Al_5O_5H_2^-$ obtained similar results with MP2/6-31+G(*d*) and B3LYP/6-311+G(3*df*,2*p*) optimizations.

CCSD(T)/6-311+G(2*d*,*p*) single-point calculations[26] on B3LYP-optimized geometries of $Al_3O_3^-$ were carried out to check for discrepancies that might be produced by higher-order correlation effects.

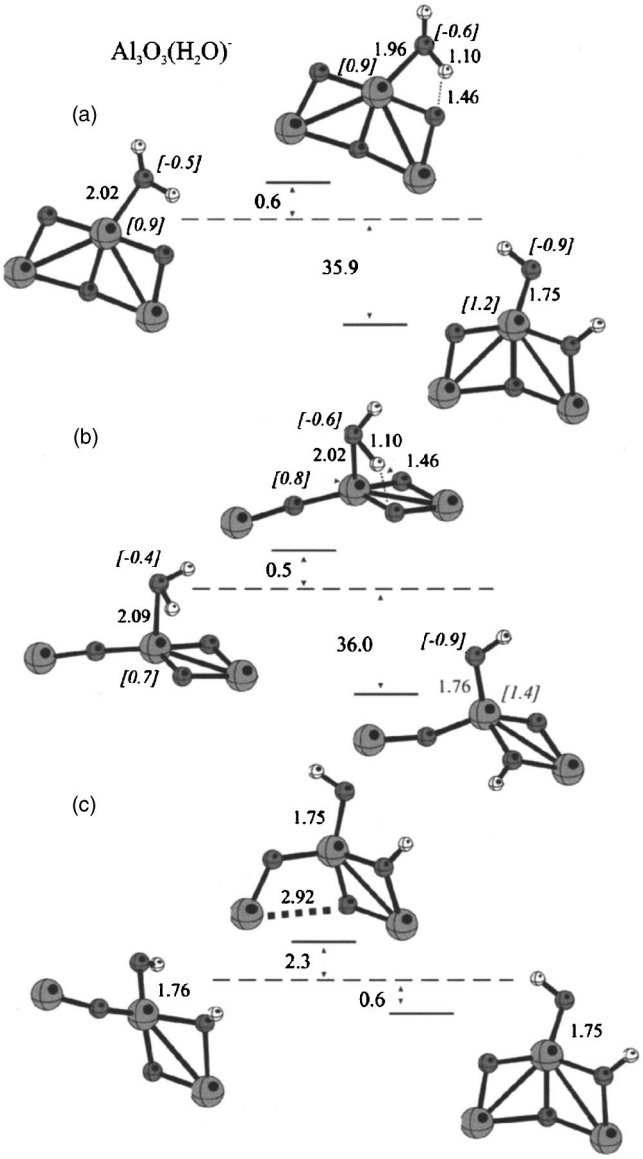

FIG. 2. B3LYP/6-311+G(2*d*,*p*) optimized structures of $Al_3O_4H_2^-$: (a) book ion-H_2O complex, dissociative adsorption product, and the transition state that lies between them, (b) kite ion-H_2O complex, dissociative adsorption product, and the transition state that lies between them, and (c) book and kite dissociative adsorption products and the transition state that lies between them. Relative energies are in kcal/mol and Mulliken atomic charges are in brackets.

Electron propagator[27] calculations on the VEDEs of the stable minima were performed in the P3 (Ref. 28) and P3+ (Ref. 29) approximations. The 6-311+G(2*df*,*p*) basis set was used, except for calculations on $Al_3O_4CH_4^-$, where the *f* functions were omitted. A modified version of GAUSSIAN03 was used for these calculations. Figures were produced with the BALL AND STICK program.[30]

RESULTS AND DISCUSSION

Stable structures and transition states

In Figs. 1–4, schematic reaction paths and energy differences obtained with the B3LYP/6-311+G(2*d*,*p*) model are shown. CCSD(T)/6-311+G(2*d*,*p*) calculations on the minima of Fig. 1 produced discrepancies for the isomeriza-

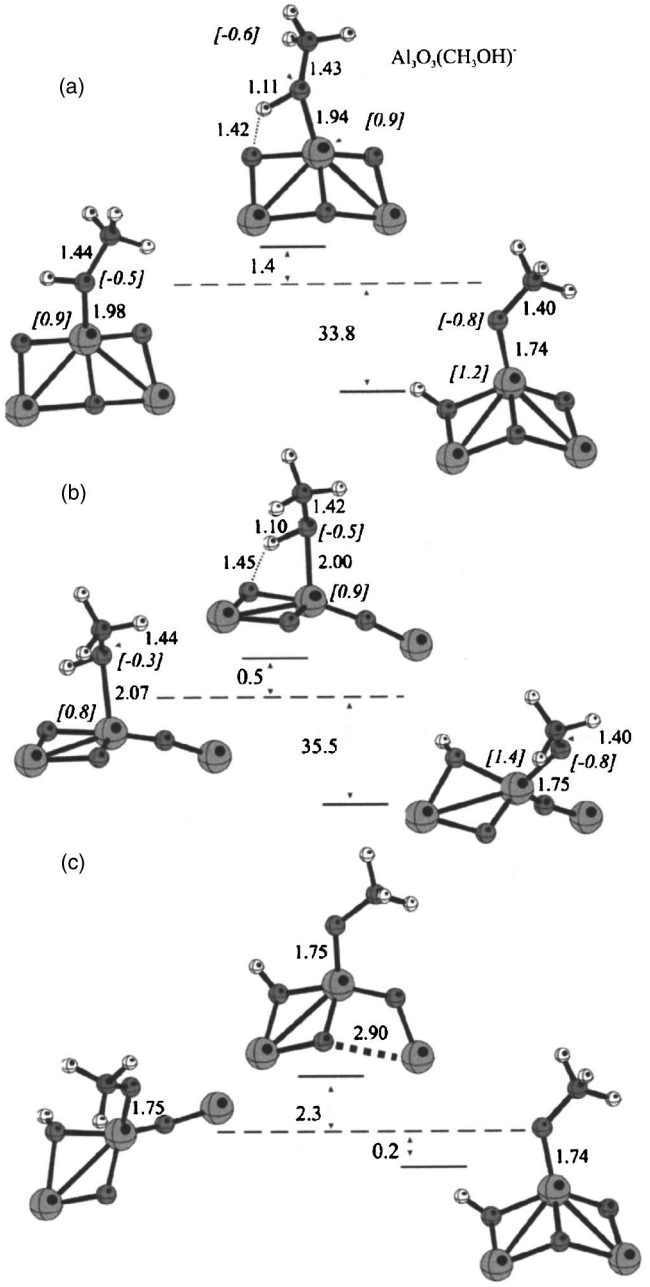

FIG. 3. B3LYP/6-311+G(2*d*,*p*) optimized structures of $Al_3O_4CH_4^-$: (a) book ion-CH_3OH complex, dissociative adsorption product, and the transition state that lies between them, (b) kite ion-CH_3OH complex, dissociative adsorption product, and the transition state that lies between them, and (c) book and kite dissociative adsorption products and the transition state that lies between them. Relative energies are in kcal/mol and Mulliken atomic charges are in brackets.

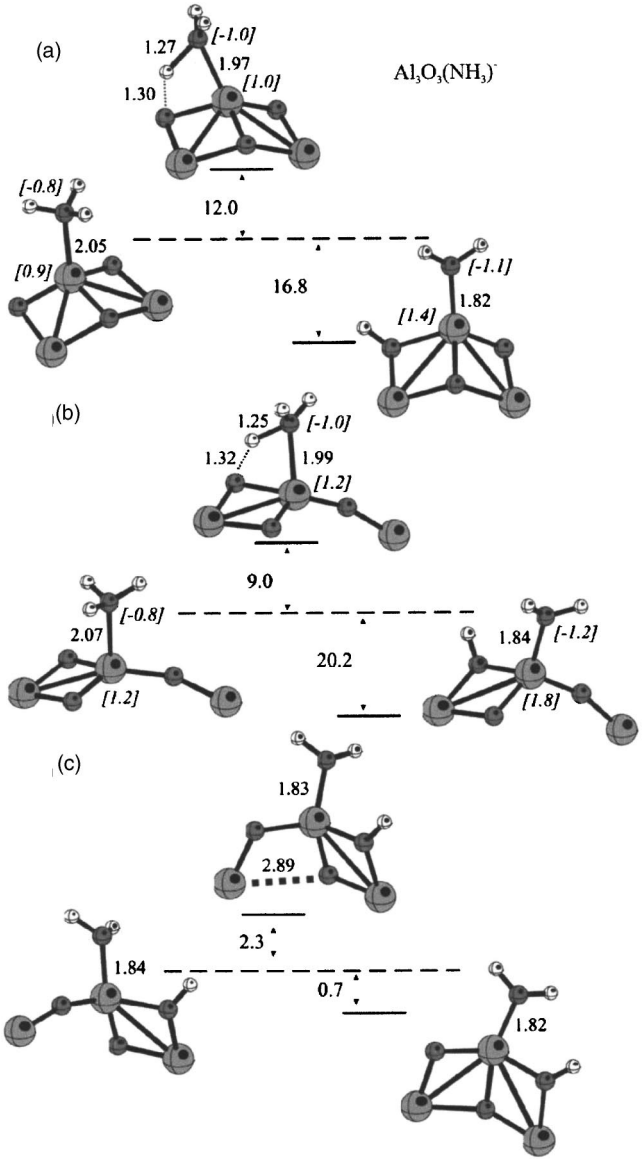

FIG. 4. B3LYP/6-311+G(2*d*,*p*) optimized structures of $Al_3O_3NH_3^-$: (a) book ion-NH_3 complex, dissociative adsorption product, and the transition state that lies between them, (b) kite ion-NH_3 complex, dissociative adsorption product, and the transition state that lies between them, and (c) book and kite dissociative adsorption products and the transition state that lies between them. Relative energies are in kcal/mol and Mulliken atomic charges are in brackets.

tion energy that are less than 1.0 kcal/mol and support the reliability of the B3LYP/6-311+G(2*d*,*p*) results in Figs. 2–4.

In a previous paper,[14] we reported density-functional and quadratic configuration-interaction calculations on Al_3O_3 and $Al_3O_3^-$. These results indicated that the book and kite isomers of $Al_3O_3^-$ have nearly identical energies. Figure 1 shows the reaction path, including a transition state. The small energy barrier (4.7 kcal/mol) implies that both isomers will be represented in the photoelectron spectrum and that isomerization occurs under the conditions of the experiments.[6,7]

Coordination complexes involving an intact water molecule, products of dissociative adsorption, and transition states that lie between these minima are summarized in Figs. 2(a) and 2(b). Energy barriers to proton transfer from the coordination complexes are very small. In contrast, the reaction energies are more than 30 kcal/mol. Bond distances between the oxygen atom of the intact water molecule and the coordinating aluminum atom become shorter after proton transfer.

Figure 2(c) schematically shows the isomerization path between the dissociative adsorption products. The two stable isomers of $Al_3O_4H_2^-$ differ in energy by 0.6 kcal/mol, but the barrier is smaller (2.3 kcal/mol) than its counterpart from Fig. 1. Das *et al.*[25] reported a somewhat larger barrier (3.1 kcal/mol) for the reaction of $Al_5O_4^-$ with water on the basis of similar computational methods.

Three conclusions follow from these results:

(a) products of dissociative adsorption have lower energies than ion-molecule complexes in which an intact water molecule is coordinated to an Al atom,
(b) the activation energy for dissociative adsorption of a water molecule via proton transfer from an anion-molecule complex is small, and
(c) there is a small barrier to isomerization from the kite structure to the book structure of $Al_3O_4H_2^-$.

The photoelectron spectrum of the anions produced by reacting $Al_3O_3^-$ with 1 molecule of methanol is similar to its water counterpart.[8] Figures 3(a) and 3(b) display the reaction paths for the book and kite isomers of $Al_3O_3^-$ with methanol. Structures produced by dissociative adsorption of the methanol are favored over those in which an intact methanol molecule is coordinated to an Al atom, with an energy difference greater than 30 kcal/mol. In the two most stable structures, a methoxy group is coordinated to the central Al atom and a proton has been added to a neighboring oxide. Barriers to proton transfer from structures with an intact methanol molecule are very small, as is the case with water. The more stable product of dissociative adsorption in Fig. 3(c) is the book form.

The dissociative adsorption structures of Fig. 3 are not global minima, but kinetically favored species that lie only ~1 kcal/mol higher than the most stable (i.e., thermodynamically favored) products, which have a hydroxide group on the central aluminum atom and a methyl group that has been transferred to a corner oxygen atom. Because the barriers to isomerization, which involve methyl group transfers, between the kinetic and the thermodynamic products are very high, the thermodynamic products are not likely to be represented in the experiments considered here.

The reaction paths of Figs. 2 and 3 are similar. The central aluminum atom is the most positively charged in all cases and is the best site for the approach of oxygen lone pairs. Whereas two well-separated peaks occur in the $Al_3O_3^-$ spectrum, the $Al_3O_4H_2^-$ and $Al_3O_4CH_4^-$ experiments yield a more complex pair of broad, overlapping humps.[8] Ground states with similar structures, low barriers to proton transfer from simple coordination complexes, and inequivalent environments for the two Al atoms that are not attacked by the water or methanol molecules account for the similarity of the $Al_3O_4H_2^-$ and $Al_3O_4CH_4^-$ spectra and for their differences with the $Al_3O_3^-$ spectrum. The product of dissociative adsorption formed by a methanol molecule and the kite isomer of $Al_3O_3^-$ also may be represented in the $Al_3O_4CH_4^-$ photoelectron spectrum.

To compare nucleophiles with oxygen and nitrogen lone pairs, reaction paths for the addition of an ammonia molecule to $Al_3O_3^-$ are considered presently. For this system, energy barriers to proton transfer shown in Figs. 4(a) and 4(b) are higher (12.0 and 9.0 kcal/mol for the book and kite, respectively) than in the other systems. Stabilization energies associated with proton transfer from the initial coordination complex are less than those for the water and methanol compounds. The Al–N bond becomes shorter after proton transfer; Al–O bonds behave similarly in the water and methanol reactions. Lower symmetry obtains in all products of dissociative adsorption. However, in the ammonia case, experimental conditions of synthesis may produce species that are insufficiently energetic to surmount the activation barriers to proton transfer, thus precluding observation of dissociative adsorption products with anion photoelectron spectra. Overcoming the lower barrier in the kite case [Fig. 4(b)] yields a product that easily rearranges to the most stable structure of Fig. 4(c). Therefore, in the presence of the kite isomer of $Al_3O_3^-$, it is necessary to overcome only the 9.0-kcal/mol barrier, not the 12.0-kcal/mol barrier of Fig. 4(a), to produce the book form of the dissociative adsorption product.

TABLE I. B3LYP/6-311+G(2*d*,*p*) reaction energies (kcal/mol).

Reaction	ΔE book	ΔE kite
$Al_3O_3^- + H_2O \rightarrow Al_3O_3^-(H_2O)$	−12.44	−12.17
$Al_3O_3^- + H_2O \rightarrow [Al_3O_2(OH)_2]^-$	−48.30	−48.19
$Al_3O_3^- + CH_3OH \rightarrow Al_3O_3^-(CH_3OH)$	−13.90	−12.45
$Al_3O_3^- + CH_3OH \rightarrow [Al_3O_2OH(OCH_3)]^-$	−47.68	−47.96
$Al_3O_3^- + NH_3 \rightarrow Al_3O_3^-(NH_3)$	−15.70	−12.08
$Al_3O_3^- + NH_3 \rightarrow [Al_3O_2OH(NH_2)]^-$	−32.46	−32.26

In a previous work,[19] the symmetry equivalence of the two corner Al atoms over which four electrons are delocalized in the book isomer of $Al_3O_3^-$ was contrasted with the inequivalence of these sites in the final product produced by the reaction of this anion with a water molecule. Two delocalized Dyson orbitals corresponding to $Al_3O_3^-$ electron detachment energies bore little resemblance to their two localized counterparts for $Al_3O_4H_2^-$. Because the corner Al atoms in the book $Al_3O_3^-(NH_3)$ ion-molecule complex and $Al_3O_3^-$ have similar coordination environments, the corresponding spectra of these two anions are likely to be similar. However, if the activation energy for the proton shift in the ammonia case is exceeded during the preparation of the anion, then the $Al_3O_3NH_3^-$ spectrum will more closely resemble those seen for the water and methanol cases.

In Table I, reaction energies are reported for the formation of coordination complexes and products of dissociative adsorption. The binding energies for the dissociation reactions of water and methanol are similar, while smaller values result for the ammonia molecule.

Vertical electron detachment energies

Table II summarizes the VEDEs that are calculated with various electron propagator approximations and also presents experimental data. Close agreement is obtained between P3+ electron propagator calculations[14,16] and the experimental peaks in the $Al_3O_3^-$ photoelectron spectrum. The variable relative intensity of the X' peak is attributed to variations in the population of the kite isomer that depend on laser fluence and on the concentration of O_2 in the He carrier gas.[6] Correlation and final-state relaxation effects, represented by discrepancies between Koopmans's theorem (KT) and P3 or P3+ data, are large and determine the order of final states for the kite isomer.

For the four structures with the formula $Al_3O_4H_2^-$, the same methods are applied. Close agreement is seen between

TABLE II. Vertical electron detachment energies (eV).

Anion	Dyson orbital	B3LYP	KT	P3	P3+	Expt.
$Al_3O_3^-$ book	Al σ^* (X^2B_2)		2.95	2.85	2.84	2.96[6]
	Al σ (A^2A_1)		3.57	3.49	3.48	3.7[6]
$Al_3O_3^-$ kite	Al apex (X'^2A_1)		2.10	2.02	2.01	2.25[6]
	O σ^* (B^2B_2)		7.20	5.73	5.30	5.2[6]
	O π^* (C^2A_2)		6.94	5.72	5.40	5.2[6]
	Al tail (D^2A_1)		6.02	6.05	6.06	
$Al_3O_4H_2^-$ book	Al σ^*	2.72	2.84	2.72	2.72	2.7–2.8[8]
	Al σ		3.91	3.80	3.80	3.8–4.0[8]
$Al_3O_3^-(H_2O)$ book	Al σ^*		2.72	2.60	2.59	
	Al σ		3.29	3.18	3.17	
$Al_3O_4H_2^-$ kite	Al apex	3.11	3.04	2.96	2.95	2.7–2.8[8]
	Al tail		5.21	5.24	5.24	
	O π^*		7.56	6.22	5.94	
	O σ^*		8.22	6.67	6.32	
$Al_3O_3^-(H_2O)$ kite	Al apex		2.14	2.04	2.03	
	O σ^*		7.12	5.61	5.21	
	O π^*		7.01	5.68	5.36	
	Al tail		5.73	5.76	5.76	
$Al_3O_4CH_4^-$ book	Al σ^*	2.74	2.88	2.70	2.69	2.75[8]
	Al σ		3.95	3.77	3.77	
$Al_3O_3^-(CH_3OH)$ book	Al σ^*		2.52	2.32	2.31	
	Al σ		3.06	2.87	2.87	
$Al_3O_4CH_4^-$ kite	Al apex	3.14	3.09	2.94	2.94	2.75[8]
	Al tail		5.26	5.22	5.22	
	O π^*		7.51	6.00	5.78	
	O σ^*		7.63	6.17	5.93	
$Al_3O_3^-(CH_3OH)$ kite	Al apex		2.07	1.90	1.89	
	O σ^*		7.05	5.44	5.04	
	O π^*		6.87	5.41	5.08	
	Al tail		5.67	5.64	5.64	
$Al_3O_3NH_3^-$ book	Al σ^*	2.61	2.73	2.60	2.60	
	Al σ		3.83	3.71	3.70	
$Al_3O_3^-(NH_3)$ book	Al σ^*	2.13	2.40	2.26	2.25	
	Al σ		2.95	2.82	2.82	
$Al_3O_3NH_3^-$ kite	Al apex	3.00	2.93	2.84	2.84	
	Al tail		5.16	5.16	5.16	
	NH_2 π		6.35	5.30	5.17	
$Al_3O_3^-(NH_3)$ kite	Al apex	1.80	1.67	1.54	1.53	
	O σ^*		6.57	5.04	4.63	
	O π^*		6.41	5.08	4.75	
	Al tail		5.56	5.57	5.57	

experimental data and the VEDEs of the product of dissociative adsorption formed by the book isomer of $Al_3O_3^-$ and a water molecule. The breadth and complexity of the spectrum allow for the possible presence of the kite isomer, which has a predicted first VEDE that is slightly higher than that of its book counterpart. Based on the results of Table II and the information presented above on transition states, it is much less likely that coordination complexes of water with either form of $Al_3O_3^-$ are contributing to the photoelectron spectrum.

Electron propagator calculations on anions produced with methanol necessitate the use of a somewhat smaller basis, which in calculations on the two isomers of $Al_3O_3^-$ yield VEDEs that are smaller than those obtained with the larger basis by less than 0.1 eV. Results for the product of dissociative adsorption with the book isomer are in excellent agreement with the experimental value. Separations between the two lowest, predicted VEDEs of the book ($\sim$1.1 eV) and kite ($\sim$2.3 eV) isomers are approximately the same as they were in the case of the anions produced with water. The possibility that the kite also contributes to the photoelectron spectrum cannot be eliminated for the methanol case either, for the experimental spectrum also is broad and complex. In contrast, the low VEDEs predicted for the coordination complexes with the book and kite isomers of $Al_3O_3^-$ imply that these structures are not represented in the photoelectron spectrum. The calculated VEDEs for the thermodynamic products of $Al_3O_4CH_4^-$ discussed above do not change by more than 0.1 eV from the values reported for the kinetic products in Table II and the Dyson orbitals show the same localization patterns on the corner aluminum.

For all structures where an intact molecule coordinates

to the book isomer of $Al_3O_3^-$, the ~0.6-eV separation between the first two VEDEs obtained in the bare anion is approximately maintained. After dissociative adsorption, this gap increases to ~1.1 eV. Larger separations of 3.1–3.3 eV are found for the kite isomer and its complexes with intact molecules. For products of the kite anion with dissociatively adsorbed molecules, the gap between the first two VEDEs is closer to ~2.3 eV.

For the ammonia case, observation of a separation of approximately 0.6 eV between well-defined peaks would imply the presence of a coordination complex comprising the book form of $Al_3O_3^-$ and an ammonia molecule. Should a broad, complex spectrum that resembles those produced with water and methanol be seen, products of dissociative adsorption are responsible. The kite and book isomers may be present simultaneously.

For the book isomer of $Al_3O_3^-$, the Dyson orbitals for the first two VEDEs consist chiefly of Al 3*s* functions on the two corner Al atoms.[14,16] In the lowest VEDE's Dyson orbital, there is an antibonding phase relationship between these two functions; a bonding relationship obtains for the second VEDE's Dyson orbital. In addition, some delocalization onto neighboring O atoms occurs and antibonding Al–O relationships are seen. Despite the formal change of point group, these symmetry-adapted descriptions remain valid when an intact molecule coordinates to the book form of $Al_3O_3^-$. A relatively small separation of ~0.6 eV between the first two VEDEs also is conserved.

After dissociative adsorption, the Dyson orbital for the lowest VEDE localizes on the corner Al that is coordinated to two oxide centers.[19] A reduced contribution with the opposite phase remains on the other corner Al. For the second Dyson orbital, the dominant contribution is made by a 3*s* function on the corner Al that has oxide and hydroxide neighbors. Delocalization on the other corner Al is reduced, but the in-phase relationship between the two Al 3*s* functions persists. In both Dyson orbitals, Al–O antibonding interactions remain. Because of the inequivalence of the coordination environments of the corner Al sites, the separation between the first two VEDEs increases to ~1.1 eV for all three product anions.

In the kite isomer of $Al_3O_3^-$, there are four VEDEs whose order is determined by correlation corrections to KT results.[14,16] For the lowest VEDE, the a_1 Dyson orbital is localized on the apex Al and it displays antibonding interactions between an Al 3*s* function and 2*p* functions on the two neighboring O atoms that are approximately aligned with the C_2 axis. The next VEDE's b_2 Dyson orbital consists chiefly of 2*p* functions on the same two O atoms that exhibit an antibonding σ^* interaction. In the a_2 Dyson orbital that corresponds to the third VEDE, the chief contributions again are found on the bridging O atoms, but now the relationship between them is π^* antibonding. Finally, in the fourth VEDE's Dyson orbital, a 3*s* function that is localized on the tail Al predominates and there is an antibonding interaction with a 2*p* function on the tail O atom. Whereas KT predictions put the latter orbital in the second position, large correlation effects for the O-centered Dyson orbitals change the order of final states. After coordination of an intact molecule, these descriptions of the Dyson orbitals and their energy ordering remain the same. In all cases, the separation between the first and second VEDEs is 3.1–3.3 eV. The second and third VEDEs are within 0.1 eV of each other. In contrast, the separation between the third and fourth VEDEs varies between 0.4 and 0.8 eV.

After dissociative adsorption occurs, the first Dyson orbital remains localized on the apex Al, but the protonation of a neighboring oxide produces a higher VEDE.[19] In contrast with the case of $Al_3O_3^-$, the kite's lowest VEDE is now larger than that of its book counterpart. With the presence of a negatively charged hydroxide, methoxide, or amide ligand residing on the central Al, the Dyson orbital that is localized on the tail Al is destabilized and now corresponds to the second VEDE. The two neutral states are separated by ~2.3 eV in all three cases. Large correlation corrections still obtain for the two remaining VEDEs that corresponded in $Al_3O_3^-$ to Dyson orbitals that are localized on the two bridge O atoms. The protonation of one of these sites localizes the Dyson orbital onto the unprotonated bridge atom. For the ammonia case, the third VEDE corresponds to a Dyson orbital whose chief contribution is the π orbital of the amide ligand and it practically coincides with the second VEDE.

No anion photoelectron spectrum has been reported yet for reaction products of $Al_3O_3^-$ and NH_3. If experimental conditions enable the coordination complexes to convert to dissociative adsorption products, the spectrum is likely to resemble that of its water counterpart. The present calculations predict that the ~0.2-eV separation between the lowest VEDEs of the book and kite isomers that was seen for the water case also remains in effect for the ammonia products. A broad spectrum of overlapping humps would not eliminate the possibility that the kite isomer is present. The clear relative stability of the dissociative adsorption products over the coordination complexes with intact NH_3 molecules suggests the likelihood of observing the former over the latter species. However, there remains a chance that anion complexes, with their relatively low VEDEs, may be observed if experimental conditions disfavor proton transfer.

Atomic charges

Mulliken charges of the attacking oxygen and nitrogen atoms and of the aluminum atom that is directly coordinated to them are shown in italics and brackets in Figs. 1–4. These charges indicate that the oxygen and nitrogen atoms are negative while the aluminum atom is positive in all the isomers. The absolute value of the charge of each atom increases after proton transfer takes place and therefore stronger ionic bonding yields shorter Al–O and Al–N distances.

CONCLUSIONS

Barriers to the dissociative adsorption of water and methanol molecules by the book and kite forms of $Al_3O_3^-$ via proton transfer in anion-molecule complexes are low. Reaction heats are highly exothermic due to the formation of strong, ionic bonds between the most highly coordinated Al atom and the O atom of the approaching molecule. Ion-molecule complexes are unlikely to persist under the usual

conditions of synthesis. The book products are slightly more stable than their kite counterparts, but barriers to interconversion are small enough to permit observation of both isomers under the conditions of recent anion photoelectron spectroscopy experiments. Somewhat larger barriers to the proton transfers that connect ion-molecule complexes to dissociative adsorption products obtain in the ammonia case. Depending on the conditions of sample preparation, it may be possible to procure $Al_3O_3^-(NH_3)$ complexes in addition to the more stable $Al_3O_3NH_3^-$ species with hydroxide and amide ligands.

The qualitative differences between spectra pertaining to $Al_3O_3^-$ and to the products formed with H_2O, CH_3OH, and potentially with NH_3 may be explained in terms of two Dyson orbitals that are distributed over the two Al centers with the least O neighbors and their corresponding VEDEs. These orbitals consist chiefly of symmetry-adapted combinations of 3*s* functions on the two corner Al atoms of the book isomer of $Al_3O_3^-$. After dissociative adsorption, these two Al atoms are in distinct coordination environments and the Dyson orbitals localize on one site or another. The separation between the first two VEDEs increases from $\sim$0.6 to $\sim$1.1 eV. Whereas the $Al_3O_3^-$ kite isomer's lowest VEDE is lower than the book's lowest VEDE by $\sim$0.8 eV, in the dissociative adsorption products the order is reversed and the separation is $\sim$0.2 eV. The small isomerization energies and low barriers between the book and kite forms of dissociative adsorption products allow the possibility that both isomers are represented in the corresponding photoelectron spectra.

ACKNOWLEDGMENTS

The authors would like to acknowledge Sara Jiménez Cortés and María Teresa Vázquez for technical support and DGSCA/UNAM (México) for providing computer time. This work was partially funded by DGAPA (No. IN107399) and CONACYT-NSF (E120.1778/2001). The National Science Foundation provided support through a grant (CHE-0135823) to Kansas State University. One of the authors (A.G.) would like to thank CONACYT for scholarship support.

[1] G. E. Brown, V. E. Henrich, W. H. Casey *et al.*, Chem. Rev. (Washington, D.C.) **99**, 77 (1999).
[2] J. R. Scott, G. S. Groenewold, A. K. Gianotto, M. T. Benson, and J. B. Wright, J. Phys. Chem. A **104**, 7079 (2000).
[3] S. B. H. Bach and S. W. McElvany, J. Phys. Chem. **95**, 9091 (1991).
[4] S. R. Desai, H. Wu, and L. S. Wang, Int. J. Mass Spectrom. Ion Processes **159**, 75 (1996).
[5] S. R. Desai, H. Wu, C. M. Rohlfing, and L. S. Wang, J. Chem. Phys. **106**, 1309 (1997).
[6] H. Wu, X. Li, X. B. Wang, C. F. Ding, and L. S. Wang, J. Chem. Phys. **109**, 449 (1998).
[7] F. A. Akin and C. C. Jarrold, J. Chem. Phys. **118**, 1773 (2003).
[8] F. A. Akin and C. C. Jarrold, J. Chem. Phys. **118**, 5841 (2003).
[9] G. Meloni, M. J. Ferguson, and D. M. Neumark, Phys. Chem. Chem. Phys. **5**, 4073 (2003).
[10] D. van Heijnsbergen, K. Demyk, M. A. Duncan, G. Meijer, and G. von Helden, Phys. Chem. Chem. Phys. **5**, 2515 (2003).
[11] E. F. Archibong and S. St-Amant, J. Phys. Chem. A **103**, 1109 (1999).
[12] T. K. Ghanty and E. R. Davidson, J. Phys. Chem. A **103**, 2867 (1999).
[13] T. K. Ghanty and E. R. Davidson, J. Phys. Chem. A **103**, 8985 (1999).
[14] A. Martínez, F. J. Tenorio, and J. V. Ortiz, J. Phys. Chem. A **105**, 8787 (2001).
[15] A. Martínez, F. J. Tenorio, and J. V. Ortiz, J. Phys. Chem. A **105**, 11291 (2001).
[16] A. Martínez, L. E. Sansores, R. Salcedo, F. J. Tenorio, and J. V. Ortiz, J. Phys. Chem. A **106**, 10630 (2002).
[17] A. Martínez, F. J. Tenorio, and J. V. Ortiz, J. Phys. Chem. A **107**, 2589 (2003).
[18] X. Y. Cui, I. Morrison, and J. G. Han, J. Chem. Phys. **117**, 1077 (2002).
[19] F. J. Tenorio, I. Murray, A. Martínez, K. J. Klabunde, and J. V. Ortiz, J. Chem. Phys. **120**, 7955 (2004).
[20] F. A. Akin and C. C. Jarrold, J. Chem. Phys. **120**, 8698 (2004).
[21] M. J. Frisch, G. W. Trucks, H. B. Schlegel *et al.*, GAUSSIAN 03, revision B.05, Gaussian, Inc., Pittsburgh, PA, 2003.
[22] A. D. Becke, J. Chem. Phys. **98**, 5648 (1993); C. Lee, W. Yang, and R. G. Parr, Phys. Rev. B **37**, 785 (1988); B. Mielich, A. Savin, H. Stoll, and H. Preuss, Chem. Phys. Lett. **157**, 200 (1989).
[23] R. Krishnan, J. S. Binkley, R. Seeger, and J. A. Pople, J. Chem. Phys. **72**, 650 (1980); T. Clark, J. Chandrasekhar, G. W. Spitznagel, and P. v. R. Schleyer, J. Comput. Chem. **4**, 294 (1983); M. J. Frisch, J. A. Pople, and J. S. Binkley, J. Chem. Phys. **80**, 3265 (1984); A. D. McLean and G. S. Chandler, *ibid.* **72**, 5639 (1980).
[24] C. Peng, P. Y. Ayala, H. B. Schlegel, and M. J. Frisch, J. Comput. Chem. **16**, 49 (1995); C. Peng and H. B. Schlegel, Isr. J. Chem. **33**, 449 (1994).
[25] U. Das, K. Raghavachari, and C. C. Jarrold, J. Chem. Phys. **122**, 014313 (2005).
[26] K. Ragavachari, G. W. Trucks, J. A. Pople, and M. Head-Gordon, Chem. Phys. Lett. **157**, 479 (1989).
[27] J. V. Ortiz, Adv. Quantum Chem. **35**, 33 (1999); J. Linderberg and Y. Öhrn, *Propagators in Quantum Chemistry*, 2nd ed. (Wiley, Hoboken, NJ, 2004).
[28] J. V. Ortiz, J. Chem. Phys. **104**, 7599 (1996).
[29] J. V. Ortiz, Int. J. of Quantum Chem. (in press).
[30] N. Müller and A. Falk, BALL & STICK 3.7.6, molecular graphics software for MacOS, Johannes Kepler University, Linz, Austria, 2000.